

Supporting Information

Mechano-Responsive Hydrogels Crosslinked by Block Copolymer Micelles

Longxi Xiao,^{1§}Jiahua Zhu,^{1§}David J. Londono,²Darrin J. Pochan,^{1,3}and Xinqiao Jia^{1,3*}

¹Department of Materials Science and Engineering, Delaware Biotechnology Institute, University of Delaware, Newark, DE 19716, USA

²DuPont Nanotechnologies, CR&D, DuPont Co., Wilmington, DE 19801, USA

³Biomedical Engineering Program, University of Delaware, Newark, DE 19716, USA

[§]These two authors contributed equally to this work.

*Corresponding author: xjia@udel.edu

1. General Information

Materials. *Tert*-butyl acrylate (*t*BA) and *n*-butyl acrylate (*n*BA) were purchased from Sigma-Aldrich (Milwaukee, WI) and were purified by passing through an inhibitor removal column (Sigma-Aldrich). Ethyl 2-bromopropionate (EBP), 2-hydroxyethyl acrylate, copper (I) bromide (98%), *N*-(3-dimethylaminopropyl)-*N'*-ethylcarbodiimide (EDC), pyrene, *N,N,N',N',N''*-pentamethyldiethylenetriamine (PMDETA), trifluoroacetic acid (TFA), ammonium persulfate (APS), tetramethylethylenediamine (TEMED), acrylamide, *N,N'*-methylene bisacrylamide (MBA), 2,2-dimethoxy-2-phenylacetophenone (DMPA) and *N*-vinylpyrrolidone (NVP) were purchased from Sigma-Aldrich (Milwaukee, WI) and were used without further purification. Deionized water was obtained through a NANOpure Diamond water purification system (Thermo Scientific, NH).

Instrumentation. ¹H NMR spectra were recorded on a Bruker AV400 spectrometer using a deuterated solvent (CDCl₃ or d₆-DMSO) containing 1% tetramethylsilane (Sigma-Aldrich) as an internal reference. Gel permeation chromatograph (GPC) was obtained on a Waters GPC (Milford, MA) system with a 2414 refractive index detector. THF were used as the mobile phase and the flow rate was maintained at 1 mL/min. Data was analyzed using the Waters Empower software by comparison to a calibration curve of narrow polystyrene standards (Polysciences, Warrington, PA). FT-IR spectra were acquired using a Thermo Nicolet Nexus 670 spectrometer equipped with a DuraSamplIR II ATR accessory (SensIR Technologies) and were analyzed with OMNIC software. The polymer powder was deposited on the silicon ATR crystal and gently pressed down for the duration of the measurement. Spectra were taken at a resolution of 4 cm⁻¹ from 550 to 4000 cm⁻¹, and an average of 128 scans was reported. A background of the clean silicon crystal was subtracted from all sample spectra. Fluorescence spectra were collected on a HORIBA Jobin Yvon SPEX Fluoromax-4 spectrofluorometer (90 °C angle geometry, 1 cm × 1 cm quartz cell). Prior to the analysis, the stock solution with a BCM concentration of 1 mg/mL was serially diluted with deionized water to 1 × 10⁻⁵ mg/mL. Steady-state fluorescence spectra of the pyrene/BCM solutions (the final concentration of pyrene was 6 × 10⁻⁷ mol/L) were recorded under the following conditions: excitation at 333 nm, slit width 3 nm for the excitation, and 1.5 nm for the emission. The intensities of the bands I₁ at 372 nm and I₃ at 383 nm were then evaluated, ratios of which were plotted versus the polymer concentration. Dynamic light scattering(DLS) data were acquired using a Malvern Zetasizer nanoZS instrument (Malvern Instruments, UK) at 25 °C with a scattering angle of 173°. Micelle solutions (concentrations ranging from 0.1 to 1 mg/mL in DI H₂O) were passed through a 0.22 μm PVDF filter prior to analysis and measurements were made in triplicate. Data were analyzed by Malvern's DTS software using a cumulant analysis with a single exponential fit. Bright field TEM imaging was performed on a JEM-2000FX microscope operating at an accelerating voltage of 200 kV. Micelle samples were prepared by applying a drop of micelle suspension (4 μL) onto a carbon-coated copper TEM grid and allowing water to evaporate under ambient condition. Afterwards, a droplet of freshly prepared aqueous solution containing saturated uranyl acetate (10 μL) was deposited onto the dried samples. The excess solution was wicked away by a piece of filter paper, and the sample was allowed to dry for TEM observation. Tensile tests were performed using a Rheometrics Dynamic Mechanical Analyzer (RSA III, TA Instruments, New Castle, DE) at 25 °C. Hydrated samples were cut into a dumbbell shape with ASTM D412-06a standardized sizes (length: 12 mm, width: 2 mm, thickness: 1-2 mm). The initial grip separation was 12 mm and the stretching speed was 100 mm/min. At least five specimens were tested for each composition. The tensile modulus (kPa) was calculated as the slope of the initial linear portion of the stress-strain curve. The stress (σ_b) and strain (ε_b) at the breaking point were also recorded.

Statistical analysis. All quantitative measurements were performed on 3-5 replicates. All values are expressed as means \pm standard deviations (SDs). Statistical significance was determined using a two-tailed student *t*-test. A *p* value of less than 0.05 was considered to be statistically different.

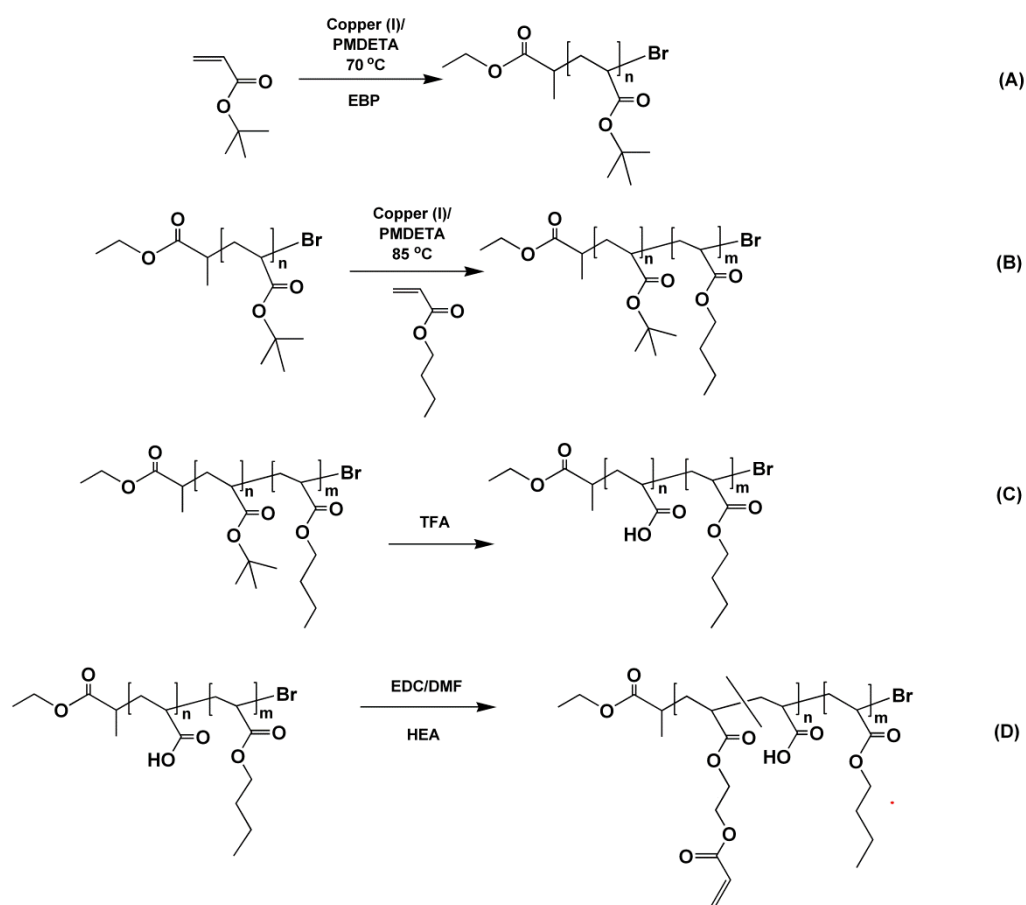
2. Polymer Synthesis and Micelle Assembly

Synthesis of poly(*tert*-butyl acrylate)-Br macroinitiator (PtBA-Br, Scheme S1A). Poly(*tert*-butyl acrylate)-Br was synthesized by ATRP following our previously reported procedure.²⁶ A pale white powdery product with ~90% yield was obtained. GPC: $M_n = 13.0$ kg/mol, $M_w/M_n = 1.22$; ¹H NMR (CDCl₃, 400 MHz): $\delta = 1.13$ (t, CH₃CH₂O-), 1.45 (m, -C(CH₃)₃), 1.52 (br, -CH₂CH-), 1.78 (m, -CH₂CH-), 2.20 (m, -CH₂CH-), 4.05 (m, CH₃CH₂O- and -CH₂CHBr, overlapping). ¹H NMR analysis indicated a polymer composition of PtBA₁₀₀-Br.

Synthesis of poly(*t*-butyl acrylate)-*b*-poly(*n*-butyl acrylate) (PtBA-*b*-PnBA, Scheme S1B). PtBA-*b*-PnBA was synthesized as previously described.²⁶ Diblock copolymers with different PnBA length was obtained by varying the reaction time from 1 to 4 h. A white powdery product with ~70% yield was obtained. GPC: $M_n = 15.2$ kg/mol, $M_w/M_n = 1.16$ for PtBA₁₀₀-*b*-PnBA₁₆, $M_n = 22.0$ kg/mol, $M_w/M_n = 1.11$ for PtBA₁₀₀-*b*-PnBA₄₀, $M_n = 24.3$ kg/mol, $M_w/M_n = 1.26$ for PtBA₁₀₀-*b*-PnBA₁₂₅. ¹H NMR (CDCl₃, 400 MHz): $\delta = 0.95$ (t, CH₃CH₂-), 1.45 (m, -C(CH₃)₃), 1.42-1.68 (m, -CH₂CH-, -CH₂CH₂CH₂CH₃ and -CH₂CH₂CH₂CH₃), 1.78 (m, -CH₂CH-), 2.20 (m, -CH₂CH-), 4.05 (m, -CH₂CH₂O-).

Synthesis of poly(acrylic acid)-*b*-poly(*n*-butyl acrylate) (PAA-*b*-PnBA, Scheme S1C). The *tert*-butyl groups was removed from PtBA-*b*-PnBA via the treatment with trifluoroacetic acid (TFA) for 48 h. The final product was obtained by removal of the solvent and TFA under vacuum (yield: 80%). ¹H NMR (DMSO-*d*₆, 400 MHz): $\delta = 0.95$ (t, CH₃CH₂-), 1.42-1.68 (m, -CH₂CH-, -CH₂CH₂CH₂CH₃ and -CH₂CH₂CH₂CH₃), 1.78 (m, -CH₂CH-), 2.20 (m, -CH₂CH-), 4.05 (m, -CH₂CH₂O-).

Polymer modification (Scheme S1D) and micelle assembly. PAA-*b*-PnBA was allowed to react with HEA to install the acrylate groups, as previously reported.²⁶ Upon completion of the reaction, the mixture was dialyzed against deionized water for 3 days in the dark to remove residual impurities and to form micelles simultaneously. ¹H NMR (DMSO-*d*₆, δ): 0.95 (t, CH₃CH₂-), 1.42-1.68 (m, -CH₂CH-, -CH₂CH₂CH₂- and -CH₂CH₂CH₂-), 1.78 (m, -CH₂CH-), 2.20 (m, -CH₂CH-), 3.85-4.40 (m, -CH₂CH₂CH₂O-, -OCH₂CH₂O- and -OCH₂CH₂O-), 5.80-6.40 (CH₂=CH- and CH₂=CH-).



Scheme S1. Synthesis of poly (acrylic acid-*graft*-hydroxyethyl acrylate)-*block*-poly (*n*-butyl acrylate) [(PAA-*g*-HEA)-*b*-PnBA]. $n=100$, $m=16$, 40 and 125.

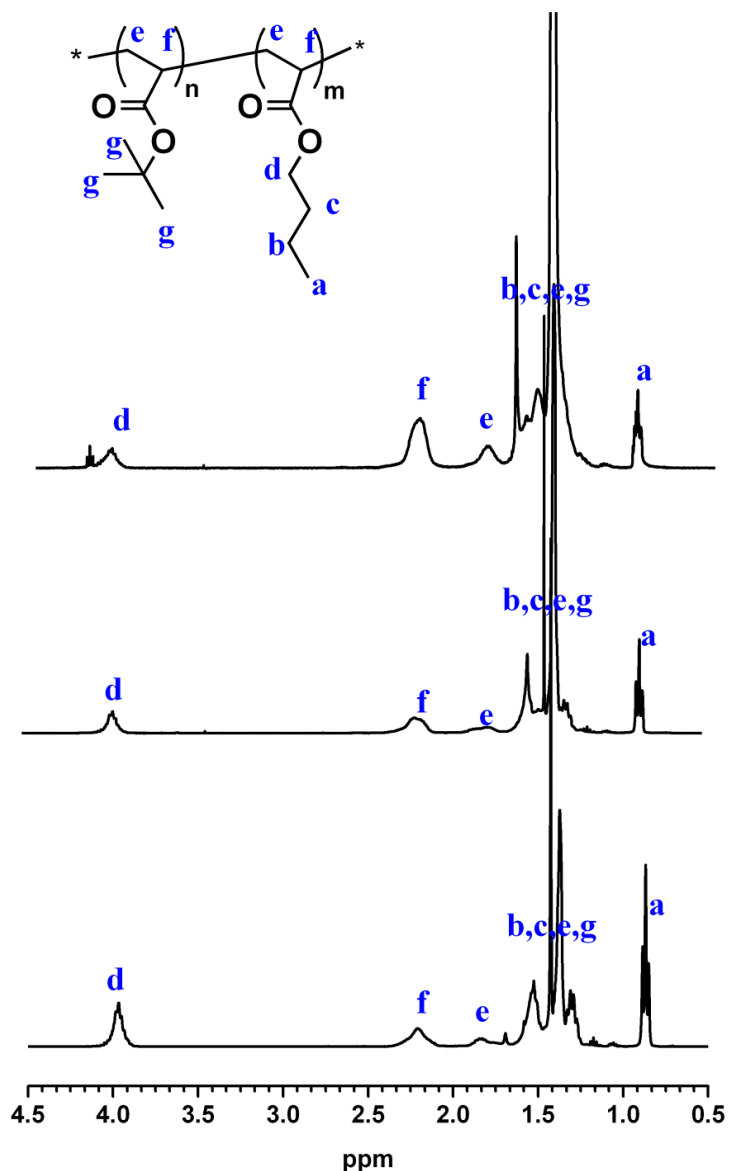


Figure S1. ^1H NMR spectra of $\text{PtBA}_{100}\text{-}b\text{-PnBA}_{16}$ (top), $\text{PtBA}_{100}\text{-}b\text{-PnBA}_{40}$ (middle) and $\text{PtBA}_{100}\text{-}b\text{-PnBA}_{125}$ (bottom) (solvent: CDCl_3).

The molecular weight of each block was calculated based on the integration of two characteristic ^1H NMR peaks from $\text{PtBA}\text{-}b\text{-PnBA}$ (a, f). Peak a resulted from the methyl protons at the end of *n*-butyl acrylate side chain ($\text{CH}_3\text{CH}_2\text{CH}_2\text{CH}_2$, designated as $A_{0.95}$) and peak f at 2.20 ppm resulted from the methine protons at both PtBA and PnBA backbone ($-\text{CH}_2\text{CH}-$, designated as $A_{2.20}$). Thus, the ratio of PnBA to PtBA can be calculated as $\frac{(A_{0.95}/3)}{A_{2.20}-A_{0.95}/3}$. Considering the ^1H NMR spectrum of $\text{PtBA}\text{-Br}$, the calculated degree of polymerization for PtBA is *ca.* 100. Therefore, $\text{PtBA}_{100}\text{-}b\text{-PnBA}_{16}$, $\text{PtBA}_{100}\text{-}b\text{-PnBA}_{40}$ and $\text{PtBA}_{100}\text{-}b\text{-PnBA}_{125}$ were obtained.

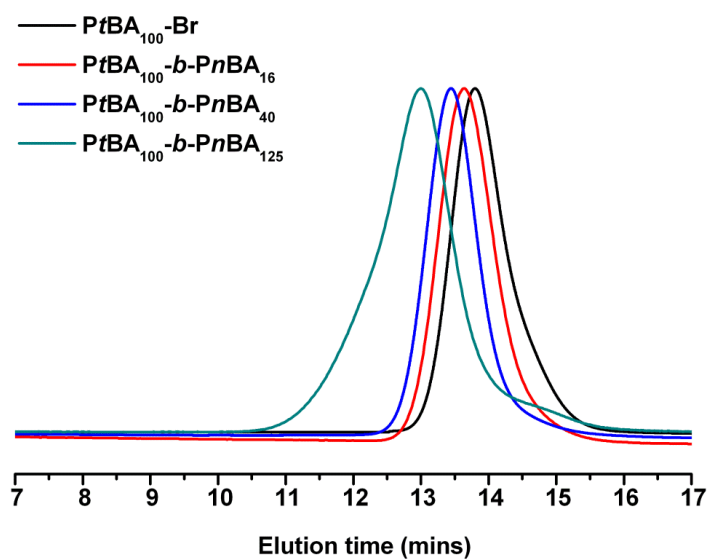


Figure S2. GPC traces of $PtBA-Br$ macroinitiator (black line, $M_n = 13.0$ kg/mol, PDI = 1.22), $PtBA_{100}-b-PnBA_{16}$ diblock copolymer (red line, $M_n = 15.2$ kg/mol, PDI = 1.16), $PtBA_{100}-b-PnBA_{40}$ diblock copolymer (blue line, $M_n = 22.0$ kg/mol, PDI = 1.11) and $PtBA_{100}-b-PnBA_{125}$ diblock copolymer (green line, $M_n = 24.3$ kg/mol, PDI = 1.26). The GPC results confirmed the progressive increase of polymer molecular weight at a longer polymerization time.

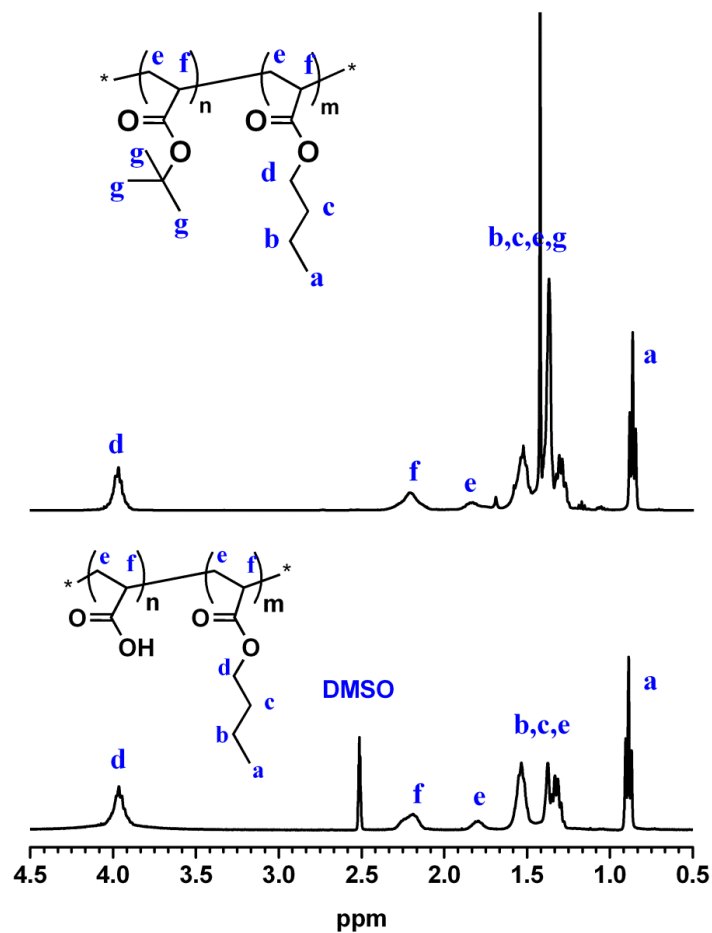


Figure S3. Representative ¹H NMR spectra of PtBA₁₀₀-*b*-PnBA₁₂₅ (top, solvent: CDCl₃) and PAA₁₀₀-*b*-PnBA₁₂₅ (bottom, solvent: d₆-DMSO).

The ¹H NMR results showed that the relative peak intensity for the methyl protons from the *t*-butyl (-C(CH₃)₃) group at 1.2~1.8 ppm to that of the methyl proton peak from the *n*-butyl group at 0.95 ppm (CH₃CH₂-) has decreased significantly. ¹H NMR analysis indicated 100% deprotection.

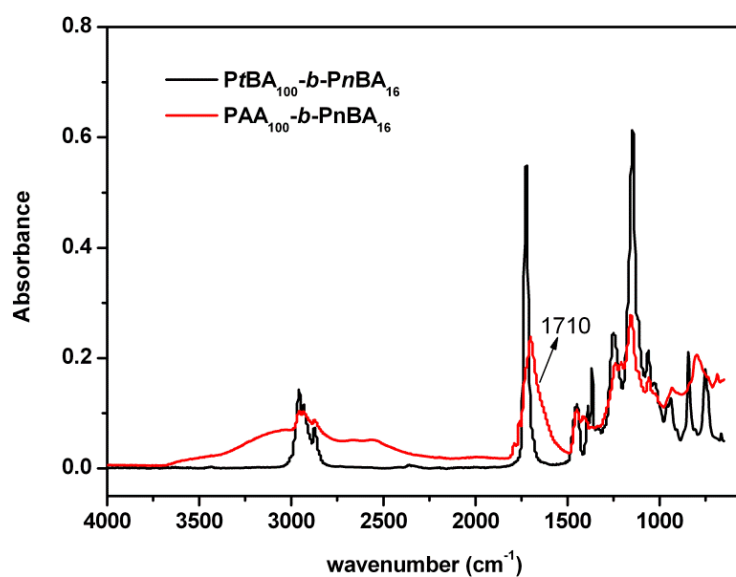


Figure S4. Representative ATR-FTIR spectra of PtBA₁₀₀-*b*-PnBA₁₆ (black) and PAA-*b*-PnBA (red).

The ATR-FTIR spectrum shows the broadening of peaks at 1710 cm⁻¹ (C=O stretch, carboxylic acid) and 2500-3500 cm⁻¹ (O-H stretch, carboxylic acid stretch) and the decreasing of peak intensity at 3000 cm⁻¹ (C-H stretching) after the removal of the *tert*-butyl groups.

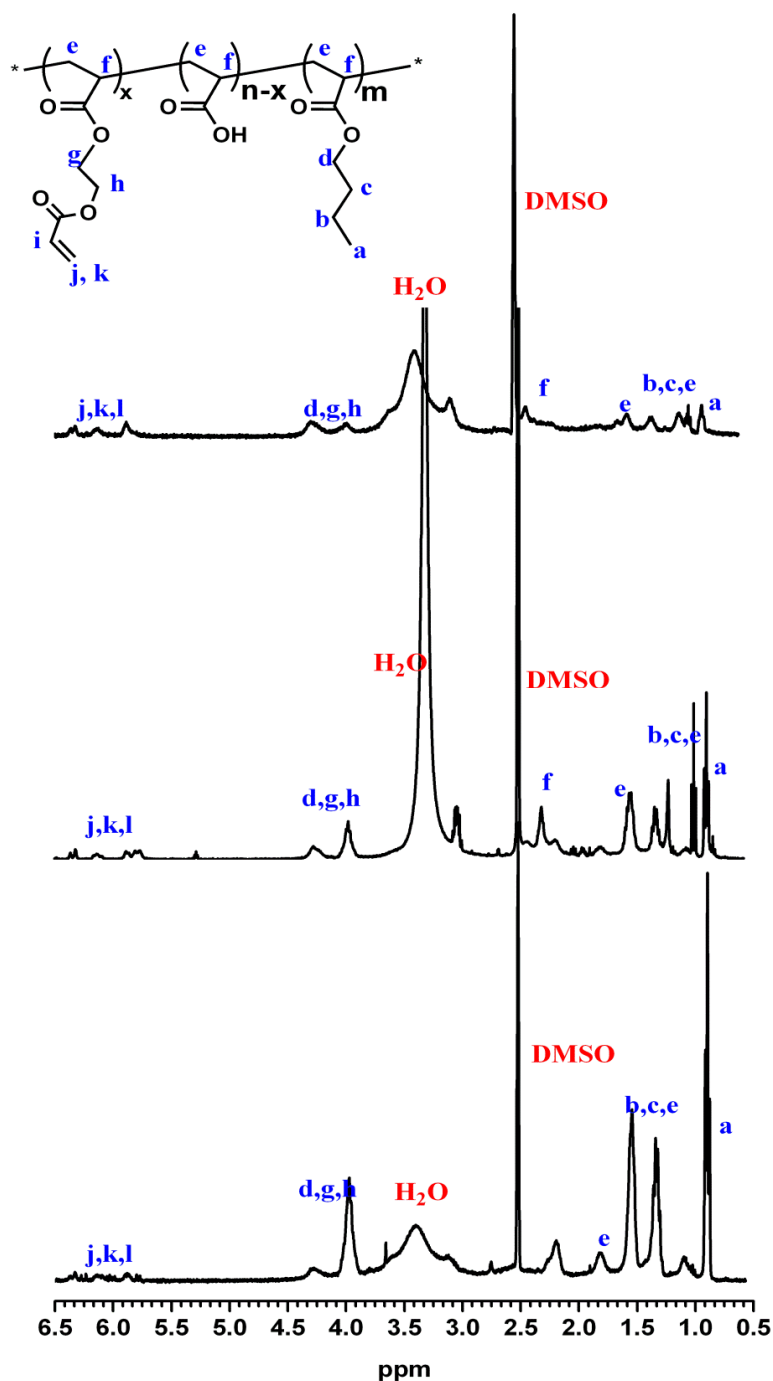


Figure S5. ^1H NMR spectra of $(\text{PAA}_{100}\text{-g-HEA}_{20})\text{-b-PnBA}_{16}$, $(\text{PAA}_{100}\text{-g-HEA}_{20})\text{-b-PnBA}_{40}$ and $(\text{PAA}_{100}\text{-g-HEA}_{20})\text{-b-PnBA}_{125}$ (solvent: $\text{d}_6\text{-DMSO}$).

The degree of modification was calculated based on the integration of three peaks at 5.80-6.40 ppm from the methylene ($-\text{CH}_2=\text{CH}-$) and methenyl protons ($\text{CH}_2=\text{CH}-$) (designated as $A_{5.80-6.40}$) and the peak at 0.95 ppm resulted from methyl protons at the end of *n*-butyl acrylate side chain ($\text{CH}_3\text{CH}_2\text{CH}_2\text{CH}_2$, designated as $A_{0.95}$) in the NMR spectra of the final product (**Figure S5**). The degree of acrylate modification, calculated from $\frac{A_{5.80-6.40}}{A_{0.95}} \times \text{DP}_{\text{PnBA}}/\text{DP}_{\text{PAA}} \times 100$, is independent of the polymer molecular weight. Thus, the final products were designated as $(\text{PAA}_{100}\text{-g-HEA}_{20})\text{-b-PnBA}_{16}$, $(\text{PAA}_{100}\text{-g-HEA}_{20})\text{-b-PnBA}_{40}$, and $(\text{PAA}_{100}\text{-g-HEA}_{20})\text{-b-PnBA}_{125}$.

3. Micelle Characterization

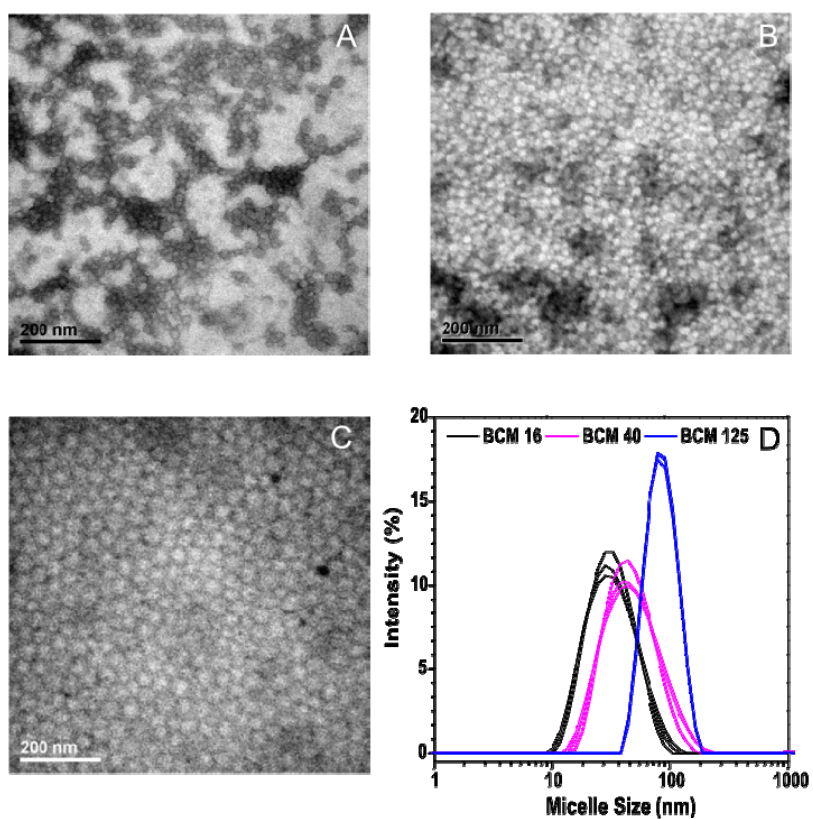


Figure S6. TEM images of BCM16 (A), BCM40 (B) and BCM125 (C) and DLS intensity profile of BCM16 (black curves), BCM 40 (pink curves) and BCM125 (blue curves) in DI H₂O (D).

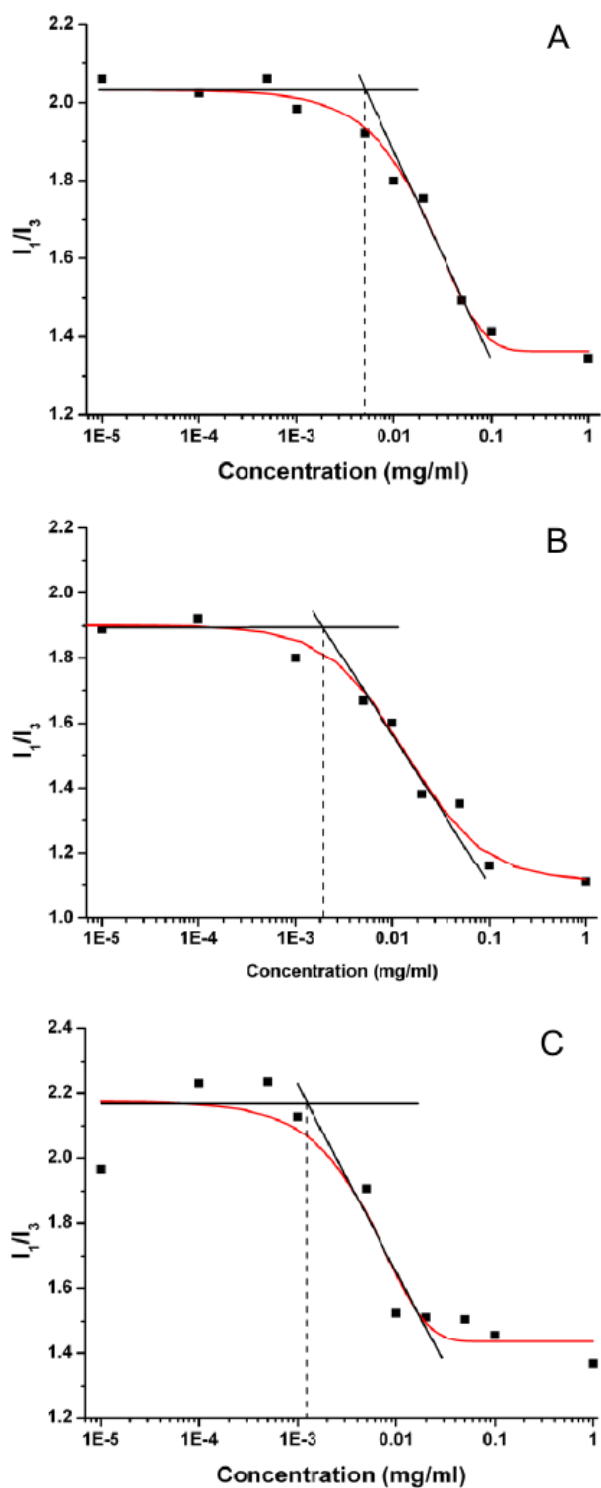


Figure S7. Critical micelle concentration (CMC), as measured by pyrene fluorescence, was found to decrease with increasing hydrophobic length, i.e. $3.3 \pm 0.9 \mu\text{g/ml}$ for BCM 16, $2.9 \pm 0.6 \mu\text{g/ml}$ for BCM 40 and $1.0 \pm 0.2 \mu\text{g/ml}$ for BCM 125.

4. Hydrogel Synthesis and Characterization

Synthesis of BCM-PAAm gels. BCM-crosslinked PAAm (BCM-PAAm) gels were prepared by free radical polymerization of AAm in the presence of various crosslinkable BCMs, following our previously reported procedure using a redox initiator pair.²⁶ Specifically, 0.5 mL of BCM solutions (15 mg/mL) was separately mixed with 250 mg of AAm in a scintillation vial. To this mixture was added 5 μ L of *N, N, N', N'*-tetramethylethylenediamine (TEMED) and 10 μ L of freshly made ammonia persulfate (APS) solution (64 mg/mL in DI water). Immediately upon mixing, the solution was rapidly loaded into a square-shaped Teflon mold (0.5"×0.5"). The mold was sealed with a Teflon lid and the reaction was allowed to occur overnight. The resultant BCM-PAAm gels were allowed to reach equilibrium swelling state prior to the mechanical tensile testing. Control gels were prepared using the same method by substituting the BCM solution with *N, N'*-methylene bisacrylamide solution at a concentration of 0.5 mg/mL.

Hydrogel sol fraction and swelling ratio. BCM crosslinked hydrogels were dried at 37 °C for two days and the initial dry weight (W_i) was recorded. After equilibrating in DI water at 37 °C for two days, the wet weight of the swollen gels (W_s) was recorded. The swollen gels were dried again at 37 °C for two days and the final dry weight (W_f) was recorded. The equilibrium swelling ratio (SW) was determined by $SW = \frac{W_s}{W_i}$, and the sol fraction (SF) was calculated according to $SF = \frac{W_i - W_f}{W_i} \times 100$. Three repeats were tested for each hydrogel composition.

Table S1. Hydrogel composition, sol fraction (SF) and equilibrium swelling ratio (SW).

Sample ID	SF (%)	SW
BCM16-PAAm	14.0 \pm 1.3	41.5 \pm 6.5
BCM40-PAAm	15.0 \pm 1.8	53.4 \pm 6.2
BCM125-PAAm	15.4 \pm 3.9	57.8 \pm 8.4

Microscopic characterization of micelle deformation. The microscopic deformation of BCM-PAAm gels was assessed via cross-sectional TEM imaging. The as-synthesized BCM16-PAAm gels were held at a constant strain of 0, 60 or 200% while being dried at ambient temperature for at least 24 h. The dry samples were then cut into ~75 nm thin sections using a Reichert Jung microtome. Prior to imaging, a drop (10 μ L) of uranyl acetate solution was added on the TEM grid for 40 seconds and images were acquired immediately after the removal of solvent.

Preparation of pyrene-loaded BCM16-PAAm gels. Pyrene was dissolved in DMSO at a concentration of (100 μ g/mL). Five microliter of pyrene/DMSO solution was added to 5 mL of pre-assembled BCM16 solution (1.5 wt%) and the mixture was stirred overnight. Pyrene-loaded BCMs were then removed by centrifugation at 14,000 rpm for 10 min using Ultra-0.5 centrifugal filter units with ultracel-100 membrane (MWCO: 100 kDa, Millipore, Billerica, MA). The fluorescent intensity of the filtrate was subsequently measured. The encapsulation efficiency (EE) was calculated based on the following equation, $EE = \frac{\text{amount of pyrene loaded into the BCMs (mg)}}{\text{amount of pyrene added initially (mg)}} \times 100$. Subsequently, pyrene-loaded BCMs were

used to crosslink PAAm as described above. The precursor solution was immediately injected into a ring-shaped Teflon mold (inner diameter of the ring: 8 mm; the outer diameter of the ring: 14 mm) for gelation. The mixture was kept in dark for overnight at room temperature to allow the reaction to complete. Hydrogels were subsequently equilibrated in PBS buffer (pH=7.4) for one day before the pyrene release study was initiated.

Evaluation of pyrene release. The ring-shaped hydrogel was immersed in 30 mL PBS buffer and was stretched using a custom-made, stepper-motor driven stretcher (**Figure S10**) which can dynamically stretch the hydrogel up to 60% strain at a constant speed of 4 mm/s and 12 cycles per minute. Three milliliter release media was withdrawn every 5 min with a 10 mL pipette and the buffer was replenished with 3 mL fresh PBS solution. Control experiments were conducted under static conditions. The amount of pyrene released was monitored using HORIBA JobinYvon SPEX Fluoromax-4 spectrofluorometer with excitation wavelength at 333 nm with 3 nm slit width and emission wavelength at 372 nm with 1.5 nm slit width.

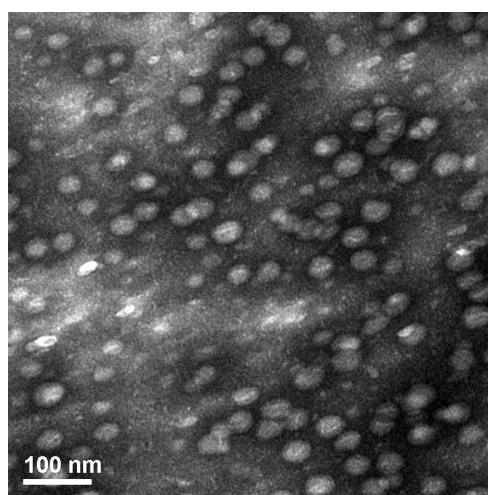


Figure S8. TEM image of BCM16-PAAm gels stretched to 60% strain.

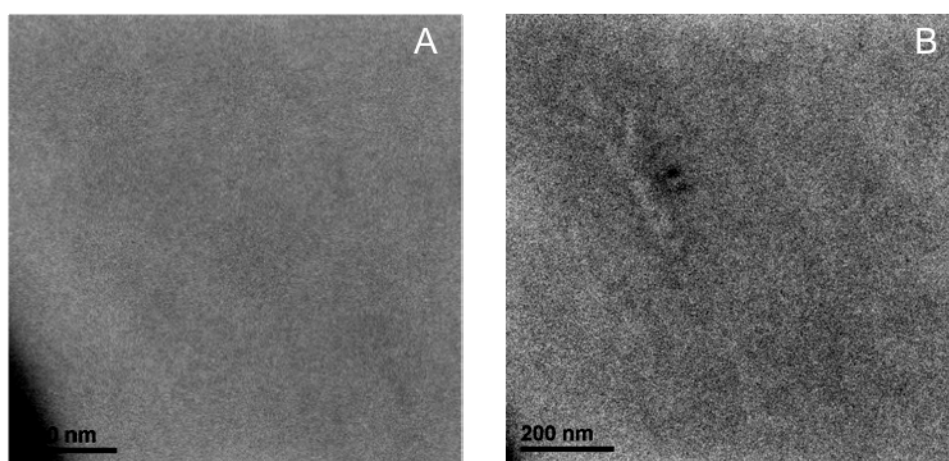


Figure S9. TEM images of PAAm gels crosslinked by N, N'-methylene bisacrylamide stretched to 0% (A) and 60% strain (B).

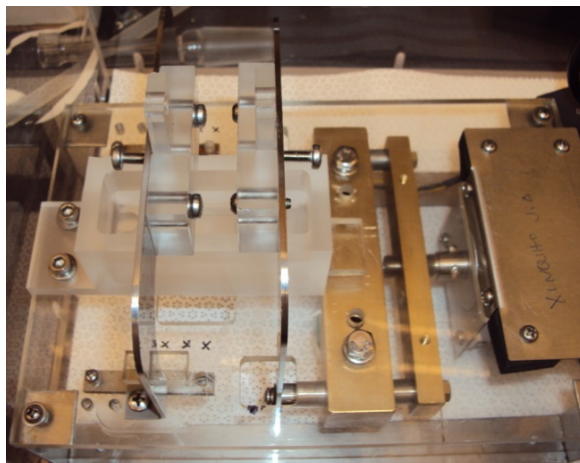


Figure S10. Digital picture of the custom designed, stepper-motor driven stretcher for the evaluation of stretch-induced pyrene release from BCM-PAAm gels.